Electronic Supplementary Material (ESI) for Nanoscale.

Supplementary Material:

Ni_2P Nanoflakes for High-Performing Urea Oxidation Reaction: Linking Active Sites to UOR Mechanism

Haipeng Liu, Shengli Zhu,* Zhenduo Cui, Zhaoyang Li, Shuilin Wu, and Yanqin Liang*
School of Materials Science and Engineering, Tianjin University, Tianjin 300072, China

*Corresponding author: slzhu@tju.edu.cn (S. L. Zhu)
*Corresponding author: yqliang@tju.edu.cn (Y. Q. Liang)

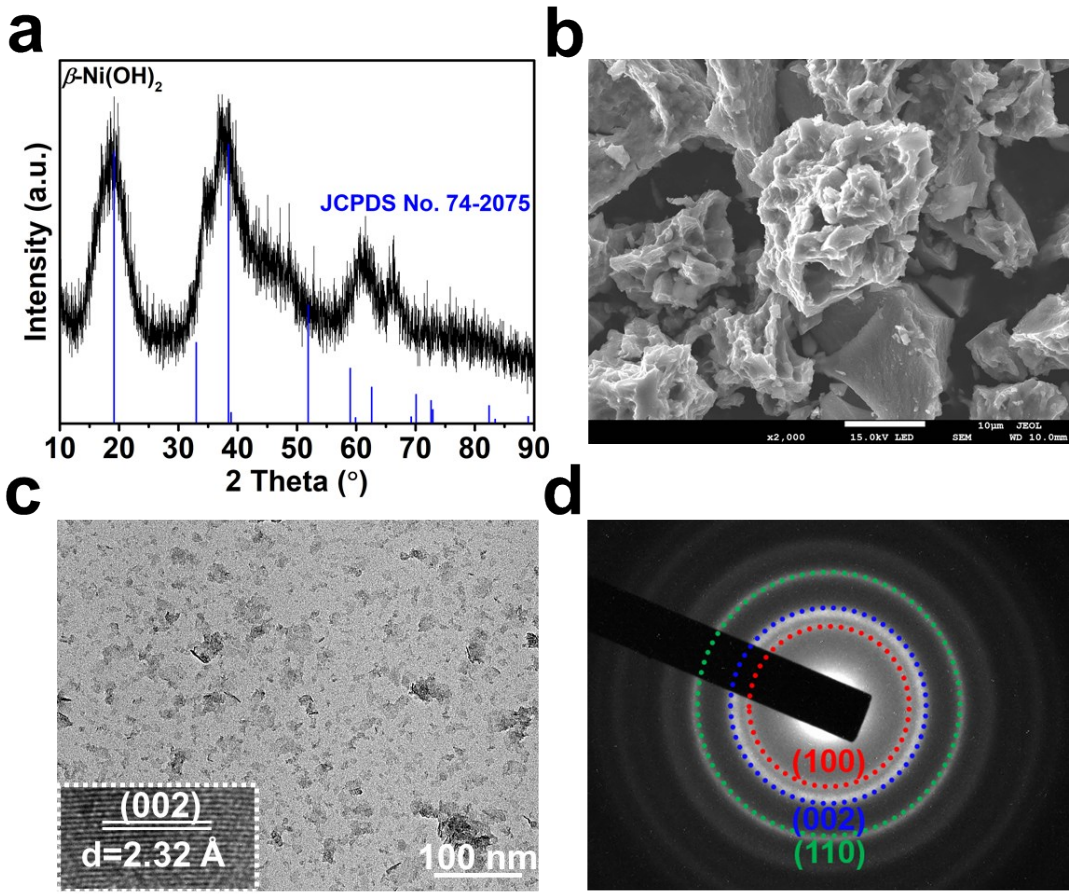

Fig. S1 Characterizations for β-Ni(OH)$_2$ nanoflakes, **(a)** XRD pattern, **(b)** SEM image, **(c)** TEM image (inset is the corresponding HRTEM image), and **(d)** SAED pattern.

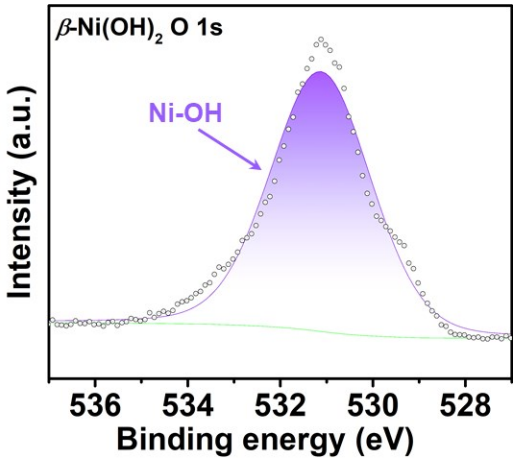

Fig. S2 O 1s XPS spectrum for β-$Ni(OH)_2$ nanoflakes.

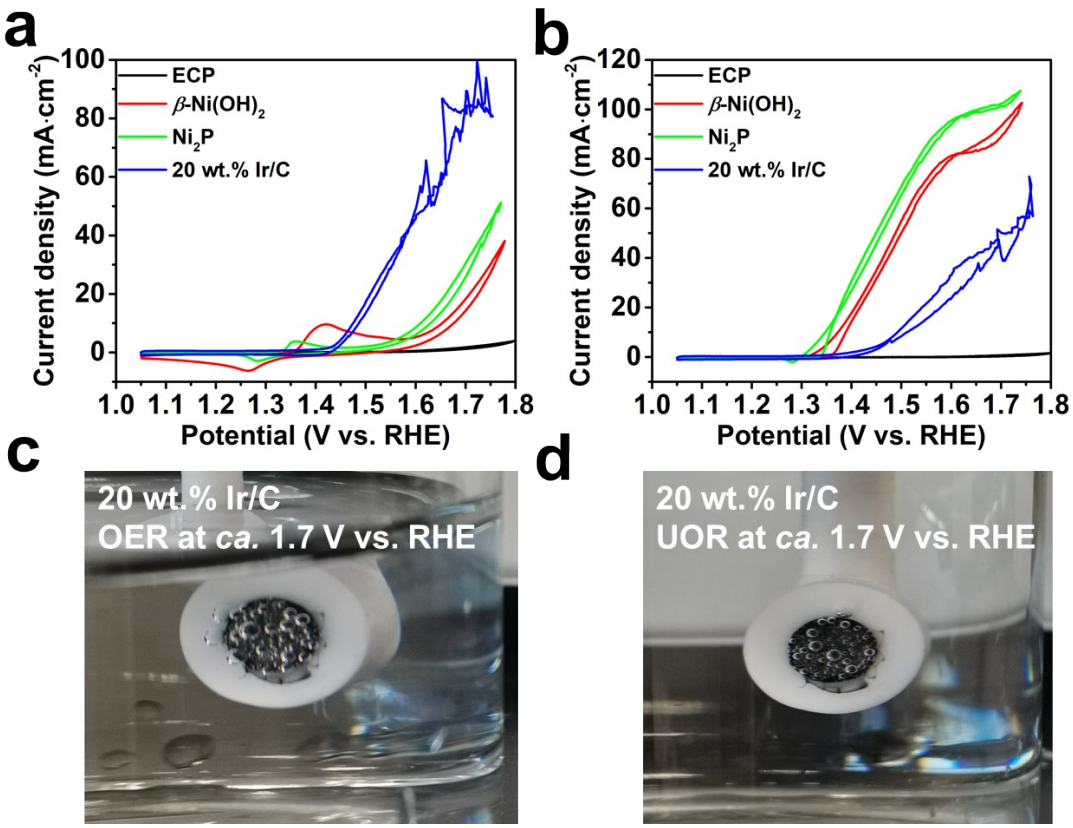

Fig. S3 Cyclic voltammetry curves in **(a)** 1 M KOH solution and **(b)** 1 M KOH with 0.5 M urea solution at a scan rate of 5 $mV \cdot s^{-1}$. **(c)** Digital picture for OER triggered by 20 wt.% Ir/C at *ca.* 1.7 V vs. RHE. **(d)** Digital picture for UOR triggered by 20 wt.% Ir/C at *ca.* 1.7 V vs. RHE.

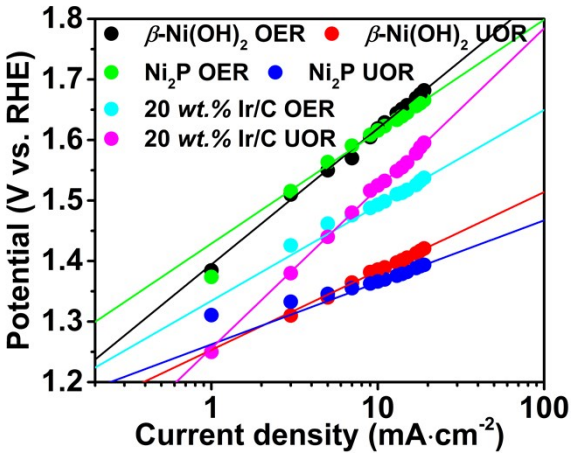

Fig. S4 Tafel slopes measured by chronopotentiometry method.

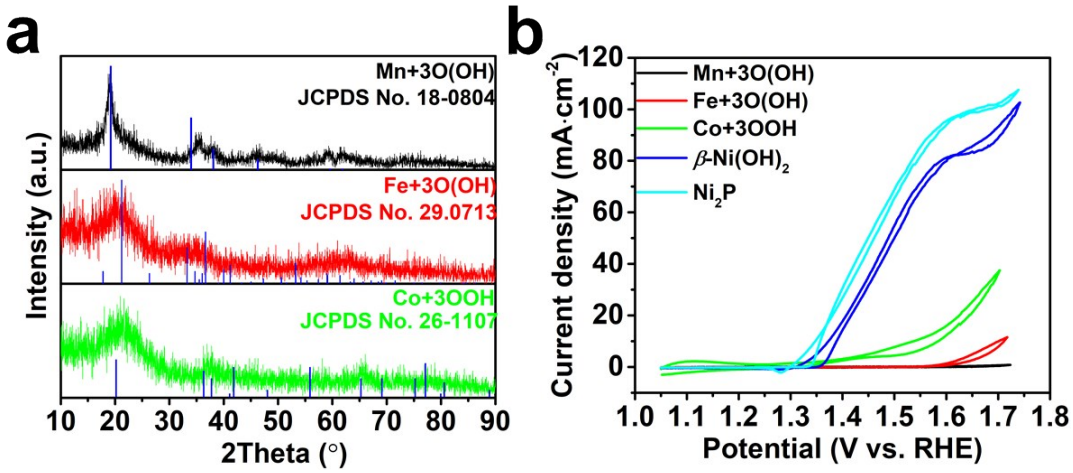

Fig. S5 (a) XRD patterns for as-synthesized non-Ni-based hydroxide catalysts. **(b)** UOR performance for non-Ni-based hydroxide catalysts, β-$Ni(OH)_2$ and Ni_2P nanoflakes.

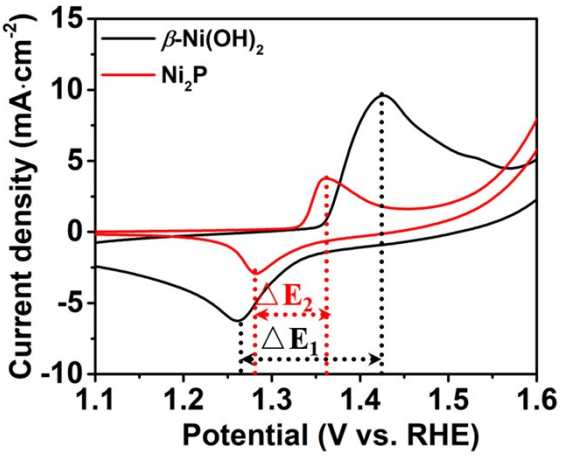

Fig. S6 Enlarged view of OER CV curves for β-$Ni(OH)_2$ and Ni_2P nanoflakes from Fig. 3a.

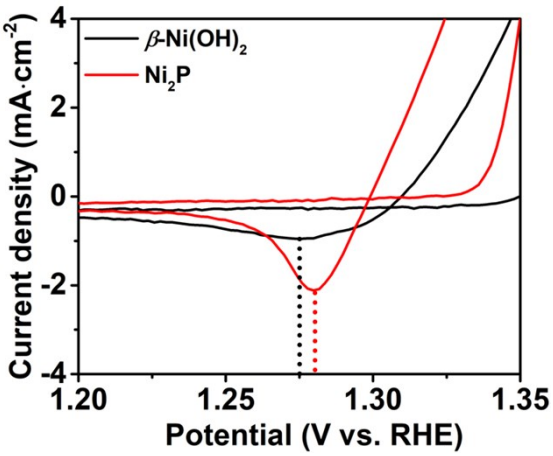

Fig. S7 Enlarged view of UOR CV curves for β-$Ni(OH)_2$ and Ni_2P nanoflakes from Fig. 3a.

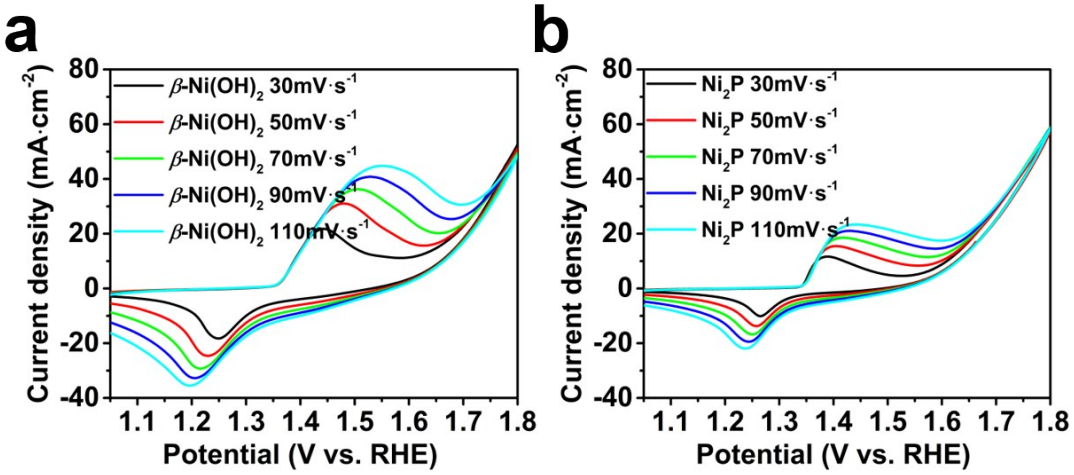

Fig. S8 CV curves for **(a)** β-$Ni(OH)_2$ nanoflakes and **(b)** Ni_2P nanoflakes in 1 M KOH at potential sweep rates of 30, 50, 70, 90, and 110 $mV \cdot s^{-1}$.

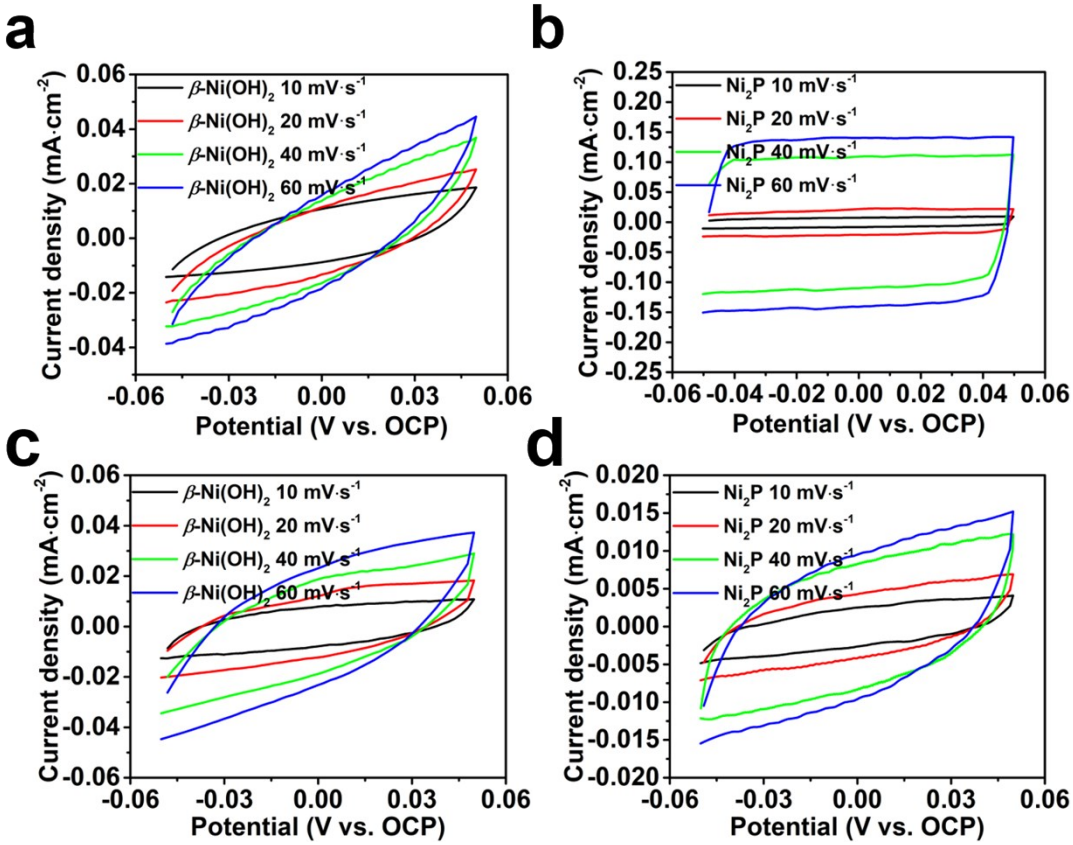

Fig. S9 Cyclic voltammetry curves for **(a)** β-$Ni(OH)_2$ nanoflakes and **(b)** Ni_2P nanoflakes measured in 1 M KOH solution, **(c)** β-$Ni(OH)_2$ nanoflakes and **(d)** Ni_2P nanoflakes measured in 1 M KOH solution with 0.5 M urea at scan rates from 10 to 60 $mV \cdot s^{-1}$.

To measure double-layer charging and discharging via CV, a potential range in which no apparent Faradaic processes occurred was determined from static CV. This range is typically a 0.05 V potential window centered at the open-circuit potential (OCP) of the system. All measured current in this non-Faradaic potential region is assumed to be due to double-layer charging and discharging[1, 2].

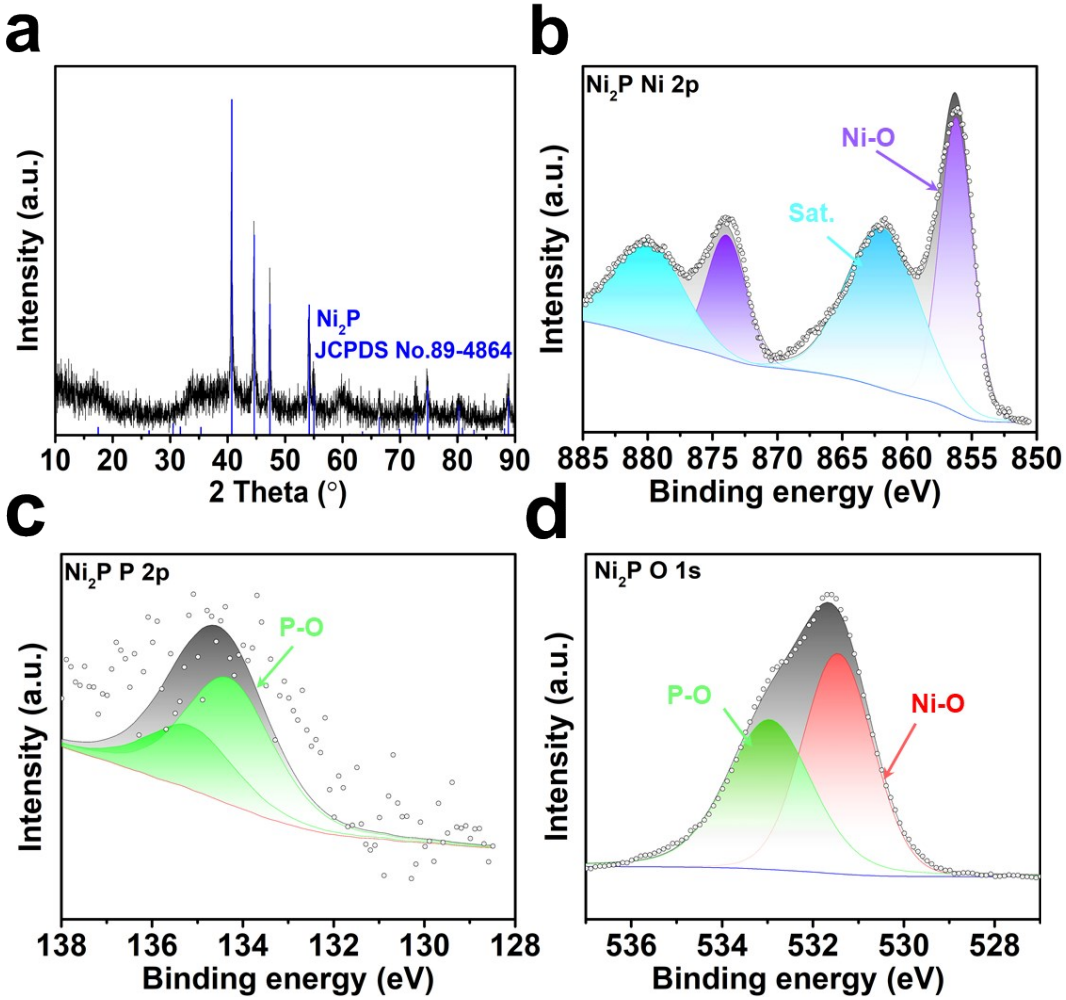

Fig. S10 Characterizations for Ni_2P nanoflakes after 250 CV cycles in 1 M KOH solution at 5 $mV \cdot s^{-1}$, **(a)** XRD pattern, XPS spectra for **(b)** Ni 2p orbital, **(c)** P 2p orbital, and **(d)** O 1s orbital.

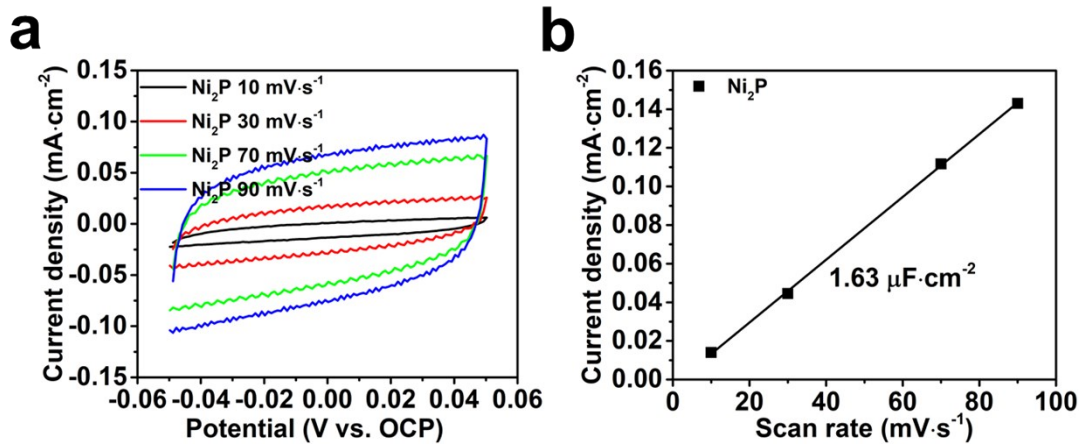

Fig. S11 (a) Cyclic voltammetry curves for Ni_2P nanoflakes measured in 1 M KOH solution. **(b)** Double layer capacitance derived from cyclic voltammetry curves in Fig. S11a.

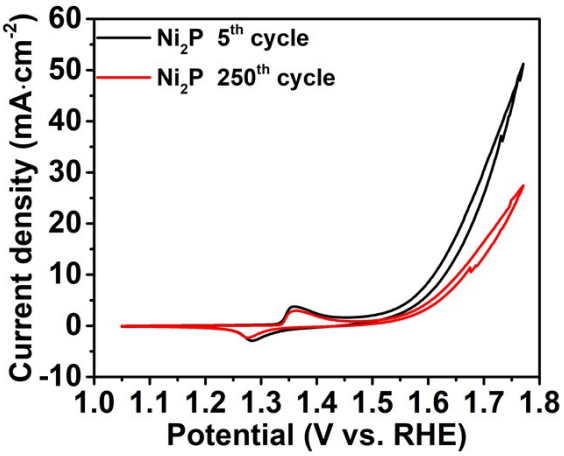

Fig. S12 5th and 250th cycle for cyclic voltammetry curves for Ni_2P nanoflakes measured in 1 M KOH solution at 5 $mV \cdot s^{-1}$.

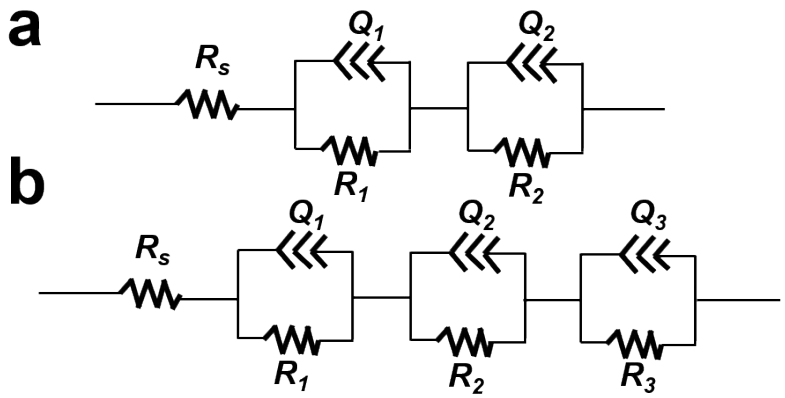

Fig. S13 Equivalent circuits used for fitting EIS spectra during **(a)** OER process, and **(b)** UOR process.

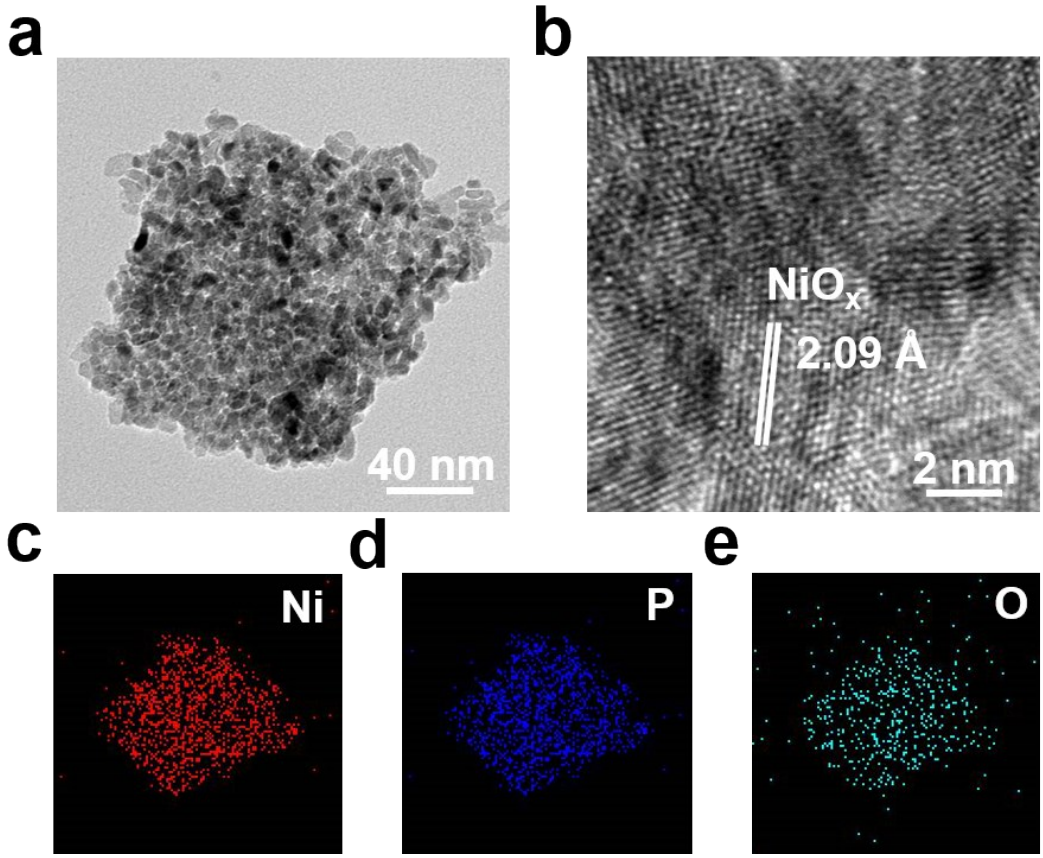

Fig. S14 (a) TEM image, **(b)** HRTEM image, **(c-e)** EDS elemental mappings for Ni_2P nanoflakes at 10 mA·cm^{-2} for 1 h in 1 M KOH with 0.5 M urea solution.

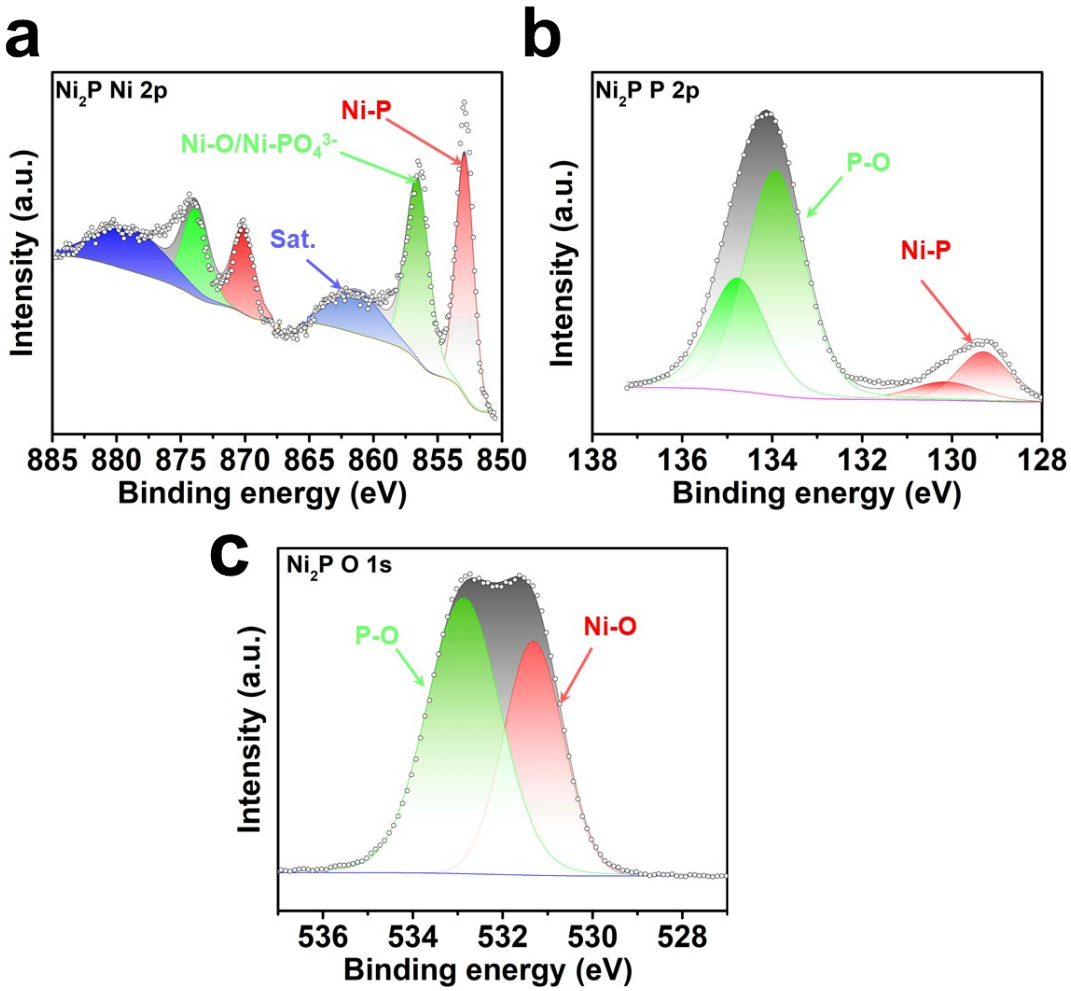

Fig. S15 XPS spectra for Ni_2P nanoflakes at 10 $mA \cdot cm^{-2}$ for 1 h in 1 M KOH with 0.5 M urea solution, **(a)** Ni 2p orbital, **(b)** P 2p orbital, and **(c)** O 1s orbital.

Table S1 Fitting results for EIS spectra.

Elements	β-$Ni(OH)_2$ OER	Ni_2P OER	β-$Ni(OH)_2$ UOR	Ni_2P UOR
R_s (Ω)	6.76	4.964	5.555	3.903
Q_1 (F)	5.721×10^{-2}	7.399×10^{-4}	3.316×10^{-2}	4.89×10^{-2}
Q_1-n	3.861×10^{-1}	6.89×10^{-1}	5.988×10^{-1}	2.721×10^{-1}
R_1 (Ω)	**2.89**	**3.528×10^{-1}**	**8.766**	**6.767×10^{-1}**
Q_2 (F)	1.693×10^{-2}	1.103×10^{-3}	8.358×10^{-4}	4.611×10^{-3}
Q_2-n	8.863×10^{-1}	8.486×10^{-1}	8.775×10^{-1}	7.167×10^{-1}
R_2 (Ω)	**11.17**	**6.521**	**10.42**	**8.934**
Q_3 (F)	-	-	5.355×10^{-2}	5.07×10^{-1}
Q_3-n	-	-	3.518×10^{-1}	9.494×10^{-1}
R_3 (Ω)	-	-	**1.215**	**1.005**

Reference

1. L. S. Bezerra and G. Maia, *J. Mater. Chem. A*, 2020, **8**, 17691-17705.

2. C. C. McCrory, S. Jung, J. C. Peters and T. F. Jaramillo, *J. Am. Chem. Soc.*, 2013, **135**, 16977-16987.